Neurotherapeutics (2020) 17:676–689
https://doi.org/10.1007/s13311-019-00803-7

ORIGINAL ARTICLE

Galantamine Inhibits $A\beta_{1-42}$-Induced Neurotoxicity by Enhancing α7nAChR Expression as a Cargo Carrier for LC3 Binding and $A\beta_{1-42}$ Engulfment During Autophagic Degradation

Ming-Wei Lin[1,2] · Yi-Hung Chen[3,4] · Han-Ben Yang[3,5] · Chi Chien Lin[5] · Shih-Ya Hung[3,6]

Published online: 10 December 2019

Abstract

Despite Alzheimer's disease (AD) being the most common neurodegenerative disorder worldwide, no FDA-approved disease-modifying treatments have been approved for this condition since 2003. Neuronal-type alpha7 nicotinic acetylcholine receptors (α7nAChRs) play an essential role in cognitive functions, binding with extracellular β-amyloid (Aβ plaques) and inhibiting Aβ-induced neurotoxicity. α7nAChRs are impaired early in the course of AD; drugs targeting α7nAChRs are being hotly pursued as a treatment of AD. Encenicline, a partial selective agonist of α7nAChR and modulator of acetylcholine, failed in phase III trials because of gastrointestinal side effects. We, therefore, evaluated the efficacy of galantamine, a positive allosteric modulator at α7nAChRs and an acetylcholinesterase inhibitor, that has been used since 2000 as first-line treatment of mild-to-moderate dementia. This study highlights an important new benefit with galantamine. We found that galantamine inhibits $A\beta_{1-42}$-induced apoptosis by activating the JNK signaling pathway, thus enhancing α7nAChR expression, and also inhibits the Akt pathway, which further increases autophagosome biogenesis and autophagy. These effects can be reproduced by α7nAChR overexpression in the absence of galantamine. Importantly, the α7 subunit protein sequence of α7nAChRs contains 3 LC3-interacting regions; our immunoprecipitation data show that α7 binds with the autophagosomal marker protein LC3. This is the first report to provide evidence showing that the cell surface receptor α7nAChR acts as a cargo carrier for LC3 binding for $A\beta_{1-42}$ sequestration to autophagosomes, suggesting a novel mechanism for the neuroprotective efficacy of galantamine in AD.

Keywords Alpha7 nicotinic acetylcholine receptor · Alzheimer's disease · Autophagy · Galantamine · Neuroprotection

Introduction

Alzheimer's disease (AD) is the most common type of dementia, accounting for an estimated 60 to 80% of cases [1]. Early clinical symptoms of AD include difficulty in remembering names and recent events, brain apathy, and depression; later clinical symptoms include impaired judgment, disorientation, confusion, behavior changes, and difficulty speaking, swallowing, and walking [2]. AD is primarily a disease of older age, roughly doubling in incidence rates every 5 years after the age of 65 years [3]. As populations increase in age worldwide, the incidence of AD is expected to more than triple by 2050, to over 115 million cases [4]. The direct societal cost of AD is second only to cancer care; an estimated $172 billion is spent annually on AD-related health-care costs in the USA [5].

Recent therapeutic approaches have been strongly influenced by 5 neuropathological hallmarks of AD: acetylcholine deficiency, glutamate excitotoxicity, extracellular deposition

✉ Shih-Ya Hung
shihyahung@mail.cmu.edu.tw

1 Department of Medical Research, E-Da Hospital/E-Da Cancer Hospital, Kaohsiung 82445, Taiwan

2 Regenerative Medicine and Cell Therapy Research Center, Kaohsiung Medical University, Kaohsiung 80708, Taiwan

3 Graduate Institute of Acupuncture Science, College of Chinese Medicine, China Medical University, Taichung 40402, Taiwan

4 Chinese Medicine Research Center, China Medical University, Taichung 40402, Taiwan

5 Department of Life Sciences, Institute of Biomedical Science, National Chung Hsing University, Taichung 40249, Taiwan

6 Division of Colorectal Surgery, China Medical University Hospital, Taichung 40447, Taiwan

of Aβ (Aβ plagues), the formation of intraneuronal neurofibrillary tangles, and neuroinflammation [6]. Acetylcholine deficiency is based on the observation that atrophy affects the cholinergic neurons in the basal forebrain projecting to the neocortex and hippocampus; this impairment is thought to underlie the progressive decline in cognitive functions in people with AD [7]. Three acetylcholinesterase inhibitors, donepezil, galantamine, and rivastigmine, are currently used in the treatment of AD, increasing levels of acetylcholine expression at cholinergic synapses by inhibiting the activity of acetylcholinesterase [6]. These agents do not prevent the progression of dementia, but they can temporarily slow the loss of cognitive function.

All eukaryotic cells use the ubiquitin–proteasome system to selectively degrade short-lived and abnormal/misfolded proteins following labeling with Lys-48-linked polyubiquitin chains and the lysosome to degrade extracellular and plasma membrane proteins transported by endocytosis and cytoplasmic components delivered by autophagy [8, 9]. Through a process of lysosomal digestion, autophagy eliminates aggregated proteins and damaged organelles in the cytoplasm [10]. Autophagy is essential in a wide variety of physiological and pathophysiological roles including energy metabolism, bacterial clearance, aging, embryonic development, red blood cell maturation and cancer, and in the pathological changes that characterize many neurodegenerative disorders, including AD, Parkinson's disease, Huntington's disease and amyotrophic lateral sclerosis [10–13]. These neurodegenerative conditions are marked by impairments in autophagy induction, autophagosome biogenesis and clearance [14].

The nAChRs belong to a family of ligand-gated ion channels consisting of various subtypes formed by 5 polypeptide subunits including α1–10, β1–4, γ, δ, and ε, all of which are activated by nicotine [15]. Neuronal-type alpha7 nicotinic acetylcholine receptors (α7nAChRs) contain 5 α7 subunits and belong to the family of ligand-gated ion channels and are expressed in cholinergic target areas (prefrontal and frontal cortices and hippocampus) [16]. α7nAChRs are involved in essential cognitive functions such as memory, thinking, comprehension, learning capacity, the ability to calculate, orientate, mastery of language, and judgment [16]. $A\beta_{1-42}$ binds to α7nAChRs with high affinity as compared to $A\beta_{1-40}$ and then internalizes the $A\beta_{1-42}$–α7nAChR complex via endocytosis [17, 18]. We have previously reported that α7nAChRs act as a carrier for extracellular $A\beta_{1-42}$ binding and further inhibit Aβ-induced neurotoxicity via autophagic degradation, an important step in Aβ detoxification [12, 13]. α7nAChR is the therapeutic target for AD drug development. Currently, encenicline (EVP-6124, MT-4666), a partial selective agonist of α7nAChRs and co-agonist with acetylcholine, is under development for the treatment of cognitive deficits in AD [19]. However, in 2015, the United States Food and Drug Administration imposed a clinical hold on encenicline following reports of gastrointestinal side effects in 2 phase III Alzheimer studies (Clinical Trial Identifier: NCT01969136 and NCT01969123) [20].

Galantamine is a phenanthrene tertiary alkaloid and first-line therapy for mild-to-moderate dementia, with proven efficacy as a modulator of nicotinic cholinergic receptors, increasing acetylcholine release [21]. As an allosteric modulator of α7nAChRs, galantamine interacts with α7nAChRs through different binding sites with acetylcholine and nicotine [22]. Nicotine protects neurons from Aβ-induced toxicity [12]. α7nAChRs and the phosphatidylinositol 3-kinase/Akt (PI3K/Akt) signaling pathway contribute to the neuroprotective effects of nicotine [23]. Atias et al. (2004) have shown that the neuroprotective qualities of galantamine in $A\beta_{1-40}$-induced apoptosis in SH-SY5Y cells is associated with α7nAChR [24]. Atias et al (2005) went on to demonstrate that the neuroprotective qualities of galantamine in $A\beta_{25-25}$-induced apoptosis are unrelated to acetylcholinesterase inhibition but instead are associated with α7nAChR and the PI3K/Akt signaling pathway in the SH-SY5Y cell line [25]. Similarly, our previous work has shown that extracellular $A\beta_{1-42}$ binding with α7nAChRs is an important step in Aβ detoxification, further enhancing the autophagic activity for Aβ clearance [12, 13]. Until now, the mechanisms underlying the effects of galantamine in autophagy regulation and α7nAChR expression have been unclear. We sought to determine what drives the neuroprotective mechanism of galantamine against Aβ neurotoxicity—whether it is via α7nAChR or autophagy. This study seeks to clarify the role of α7nAChR and autophagy in $A\beta_{1-42}$-induced neurotoxicity. Despite many important insights into this disease from the last 20 years of research, no disease-modifying treatments have emerged for AD [6]. Expanding on the results of our previous research [12, 13], this study details how galantamine mediates autophagy, which may provide important leads for new drug development.

Materials and Methods

Reagents

Galantamine hydrobromide from *Lycoris* sp. and the citrate salt of methyllycaconitine (MLA) were purchased from Sigma-Aldrich (St. Louis, MO); human $A\beta_{1-42}$ peptide was purchased from AnaSpec (Fremont, CA).

SH-SY5Y Cell Culture

SH-SY5Y cells were maintained in a 5% CO_2 incubator at 37 °C in complete medium containing Ham's F12 nutrient mixture/minimum essential medium, 10% heat-inactivated fetal bovine serum (HyClone, South Logan, UT), 4500 mg/L glucose, 1% antibiotic–antimycotic (Thermo Fisher Scientific, Waltham, MA), and 1% non-essential amino acids (Thermo Fisher Scientific).

MTT

Cell cytotoxicity of galantamine was assessed by MTT (3-(4,5-dimethylthiazol-2-yl)-2,5-diphenyltetrazolium bromide) cell proliferation assay (Thermo Fisher Scientific). Briefly, 5×10^4 cells were seeded in 96-well plates in complete medium (100 μL) overnight and then treated with galantamine. After 24 h, cell viability was measured by MTT assay with a microplate ELISA reader at 550 nm.

Western Blot

Protein levels of α7nAChR, α3nAChR, microtubule-associated protein 1 light chain 3 (LC3), p62 (also known as sequestosome 1), Beclin 1, Atg3, Atg4B, Atg5, Atg7, PTEN-induced kinase 1 (PINK1), DJ-1, Bcl-2-associated X (Bax), and poly(ADP-ribose)polymerase (PARP) were determined by Western blot, using glyceraldehyde 3-phosphate dehydrogenase (GAPDH) or β-actin as the internal control. Cells were homogenized in radioimmunoprecipitation assay buffer containing 1% protease inhibitor cocktail and 1% phosphatase inhibitor cocktail solutions (both purchased from Hycell, Taipei, Taiwan). Protein concentrations of each sample were determined using a BCA protein assay kit (Thermo Fisher Scientific). Aliquots containing 20 to 40 μg protein were separated by SDS-PAGE using 10 to 15% resolving gel under reducing conditions and electrotransferred to Immun-Blot® PVDF membranes (BioRad, Hercules, CA). After blocking with 5% nonfat milk in TBS-T (0.5% Tween 20 in 20 mM Tris and 137 mM NaCl) for 1 h at room temperature, PVDF membranes were incubated overnight at 4 °C with anti-α7nAChR (Novus, St. Charles, MO; NBP1-80092), anti-α3nAChR (abcam, Cambridge, UK; ab24666), anti-LC3 (GeneTex, Irvine, CA; GTX127375), anti-p62 (GeneTex, GTX100685), anti-Beclin 1 (Cell Signaling Technology, Danvers, MA; 3495), anti-Atg3 (Cell Signaling Technology, 3415), anti-Atg4B (Novus, NBP2-24709), anti-Atg5 (Cell Signaling Technology, 12994), anti-Atg7 (Cell Signaling Technology, 8558), anti-PINK1 (Cell Signaling Technology, 6946), DJ-1 (Cell Signaling Technology, 5933), anti-PARP (GeneTex, GTX100573), anti-Bax (Elabscience, Houston, TX; E-AB-13814), anti-β-actin (ProteinTech, Rosemont, IL; 60008), or anti-GAPDH (ProteinTech, 60004) primary antibody diluted in TBS-T at 4 °C overnight. The PVDF membranes were then incubated for 1 h at room temperature with horseradish peroxidase (HRP)-conjugated secondary antibody (1:10,000; Santa Cruz Biotechnology, Dallas, TX; sc-2004 or sc-2005). Protein bands were detected using the ECL Western blot substrate kits (Thermo Fisher Scientific) and ImageQuant LAS 4000 mini (GE Healthcare Life Sciences, Pittsburgh, PA) and then estimated by Fusion software (VilBER, Collégien, France).

Immunofluorescence Staining and Colocalization Analysis

For autophagosome studies, SH-SY5Y cells (1.8×10^5) were seeded into 24-well plates and cultured in 500 μL of complete medium overnight. After 4 h of galantamine treatment, the cells were fixed using 10% formalin and blocked/permeabilized with 10% bovine serum albumin/0.5% Triton X-100, then stained with mouse monoclonal antibody against LC3 (1:500; Santa Cruz Biotechnology, sc-376404) followed by Alexa-543-conjugated goat anti-mouse secondary antibody (1:1000, Thermo Fisher Scientific, A-11003). SH-SY5Y-pCDNA3.1-α7nAChR-C5 cells were used for labeling of the autophagosomes and α7nAChR. After fixation and blocking/permeabilization, the mouse LC3 antibody (1:500; Santa Cruz Biotechnology, sc-376404) and rabbit α7nAChR antibody (1:500; Novus, NBP1-80092) were added into cells overnight at 4 °C, then with Alexa-488-conjugated goat anti-rabbit secondary antibody (1:1000, Thermo Fisher Scientific, A-11008) and Alexa-543-conjugated goat anti-mouse secondary antibody (1:1000, Thermo Fisher Scientific, A-11003). Confocal images were obtained using excitation wavelengths of 488 nm (for Alexa-488) or 543 nm (for Alexa-543) by Leica confocal microscope (TCS SP8, Leica, Wetzlar, Germany).

Evaluation of Apoptotic Neurons by Hoechst 33342 Staining and ATP Production

To investigate the effect of Aβ-induced neuronal apoptosis, SH-SY5Y cells were seeded at a density of 5×10^4/well in 48-well culture plates in 150 μL of culture media and treated with 30 μM $A\beta_{1-42}$ in the presence or absence of galantamine (1 μM) or the α7nAChR antagonist MLA (10 nM) for 48 h. Cultures were then stained with Hoechst 33342 (10 μM; Thermo Fisher Scientific) for 10 min at room temperature. Hoechst-positive cells were obtained randomly from 3 fields of 24-well plates using a fluorescence microscope at × 200 magnification and then counted blindly as previously described [12]. The average was calculated by the percentage of Hoechst-positive cells/bright field cells obtained from 3 to 6 experiments. ATP production of cells was measured by an ATP colorimetric assay kit (BioVision, San Francisco, CA) in a microplate reader, according to the manufacturer's protocol.

α7nAChR Stable Expression and Transient Knockdown

For α7nAChR stable expression, we used a DNA synthesis service (GENEWIZ, South Plainfield, NJ) to produce α7nAChR cDNA containing the 5′XhoI enzyme digestion site, the 5′UTR sequence (CGGACTCAAC), the 1509 base-pair CDS of α7nAChR (accession: NM_000746.5, CDS: 113-1621 base-pair), and the 3′ApaI enzyme digestion site.

The synthesized DNA was ligated into a pCDNA3.1-positive plasmid (Thermo Fisher Scientific) to form the pCDNA3.1-α7nAChR construct (Fig. 5a). SH-SY5Y cells were transfected with pCDNA3.1-α7nAChR or pCDNA3.1-His (as control) using 0.1% lipofectamine 2000 reagent (Thermo Fisher Scientific). The culture medium was replaced with 600 μg/mL neomycin (G418, Amimed, London, UK)-supplemented complete culture medium 48 h after transfection. The culture medium containing G418 was changed once weekly. Four to 6 weeks later, 12 stable clones were isolated and analyzed by real-time polymerase chain reaction and Western blot for α7nAChR expression. Two to 3 stable clones of SH-SY5Y/pCDNA3.1-α7nAChR or SH-SY5Y/pCDNA3.1-His were selected for the following studies. For α7nAChR transient knockdown, we used 2 vector-based short hairpin RNAs (pLKO1-shα7nAChR-A and pLKO1-shα7nAChR-B) to knockdown α7nAChR in SH-SY5Y cells. Twenty-four hours after shRNA transfection, puromycin (4 μg/mL) was added for another 48 h to select the knockdown cells for the following studies. The shα7nAChR-A and shα7nAChR-B target sequence to α7nACR mRNA (NM_000746.4) are GCAAATGTCTTGGACAGATCA and TGCAGATCATGGACGTGGATG, respectively.

Immunoprecipitation

To test the protein–protein interaction of α7nAChR and LC3, each underwent immunoprecipitation by anti-α7nAChR (Novus, NBP1-80092) or anti-LC3 (GeneTex, GTX127375) antibody. SH-SY5Y/pCDNA3-α7nAChR stably expressing cells were seeded at a density of 6×10^6 cells/10-cm dish with 7 mL of complete medium 24 h before being harvested for protein extraction. In this study, 1 μg of anti-α7nAChR or anti-LC3 antibody was conjugated to 50 μL of protein A or protein G magnetic beads (Thermo Fisher Scientific) for 60 min, then 1 mg of total protein from each cell clone was added to immunoprecipitate the target protein for 4 h on a rotator at 4 °C. Unbound protein was then washed out using NP-40 containing cell lysis buffer on a magnetic rack. After elution, the immunoprecipitated protein was collected for Western blot analysis. In Western blot, we used EazyBlot HRP-conjugated anti-rabbit or anti-mouse IgG (GeneTex, GTX221666-01 or GTX221667-01) as the secondary antibody to avoid the interference of IgG heavy chains and light chains.

Statistics

Values are expressed as the mean ± the standard error of the mean (SEM) and were statistically analyzed using the 1-way analysis of variance with Dunnett's *post hoc* test by GraphPad Prism 5 to determine the significance of any between-group differences. The threshold for statistical significance was defined as $p < 0.05$.

Results

Galantamine Enhances α7nAChR But Not α3nAChR Expression in SH-SY5Y Cells

As an allosteric potentiator ligand of nAChRs, galantamine interacts with nAChRs through binding sites that are distinct from those used by acetylcholine and nicotinic agonists and antagonists to enhance the sensitivity to acetylcholine [22]. We have previously shown that α7nAChR acts as a carrier to bind with extracellular $A\beta_{1-42}$, which further inhibits Aβ-induced neurotoxicity via autophagy [12, 13]. In this study, we initially analyzed the dose–response effect of galantamine on neurotoxicity and α7nAChR expression. Cell viability data obtained from the MTT assay show that galantamine was not neurotoxic in the range of 0.1 to 10 μM when applied to SH-SY5Y cells for 24 h (Fig. 1a). Western blot results show that galantamine dose-dependently (0.1-1 μM) enhanced α7nAChR but not α3nAChR expression in cells treated for 24 h (Fig. 1b).

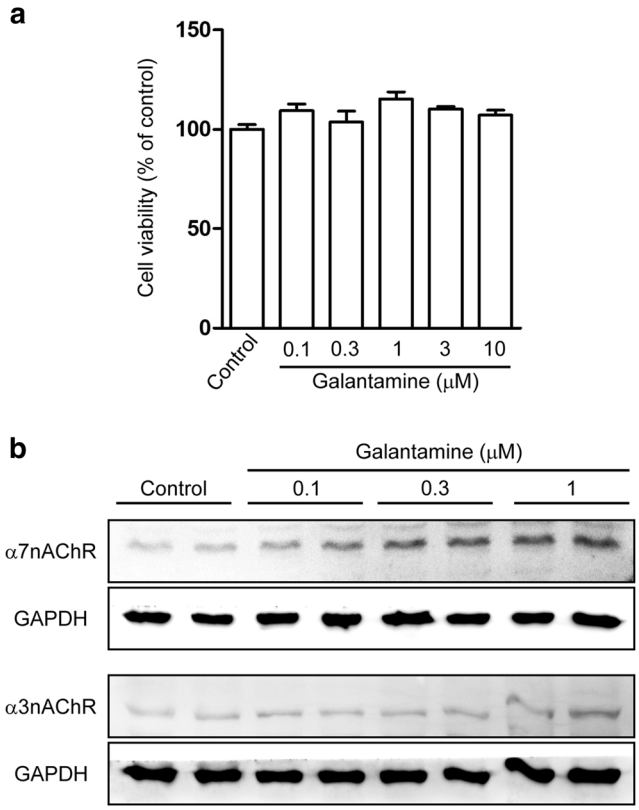

Fig. 1 Galantamine enhances α7nAChR but not α3nAChR expression in neurons. (a) At 24 h after treating the neuronal cell line SH-SY5Y with galantamine (0.1-10 μM), MTT results revealed no effects of galantamine on cell viability as compared to control. (b) Western blot results show that 24 h of galantamine treatment enhanced α7nAChR, but not α3nAChR, expression in SH-SY5Y cells. Data are expressed as mean ± SEM.

Galantamine Activates the MAPK/JNK Signaling Pathway to Enhance α7nAChR Expression and Inhibits the PI3K/Akt Signaling Pathway to Activate Neuronal Autophagy

This study shows that, at nontoxic doses, galantamine enhances α7nAChR expression in neurons. Galantamine appears to protect SH-SY5Y cells against $A\beta_{25–35}$ neurotoxicity via the α7nAChR and PI3K/Akt pathway, a manner that is unrelated to acetylcholinesterase inhibition [25]. Our Western blot results show that galantamine (0.03-1 μM for 4 h) dose-dependently inhibited PI3K/Akt (phospho-Akt↓) and activated MAPK/p38 (phospho-p38↑) and MAPK/JNK (mitogen-activated protein kinase/c-Jun NH2-terminal kinase; phospho-JNK↑), but had no effect on the MAPK/Erk (mitogen-activated protein kinase/extracellular-signal-regulated kinase) signaling pathways in SH-SY5Y cells (Fig. 2a). Using inhibitors to block these signaling pathways, we found that the JNK inhibitor SP600125 (10 μM) not only inhibited endogenous α7nAChR expression but also antagonized galantamine-

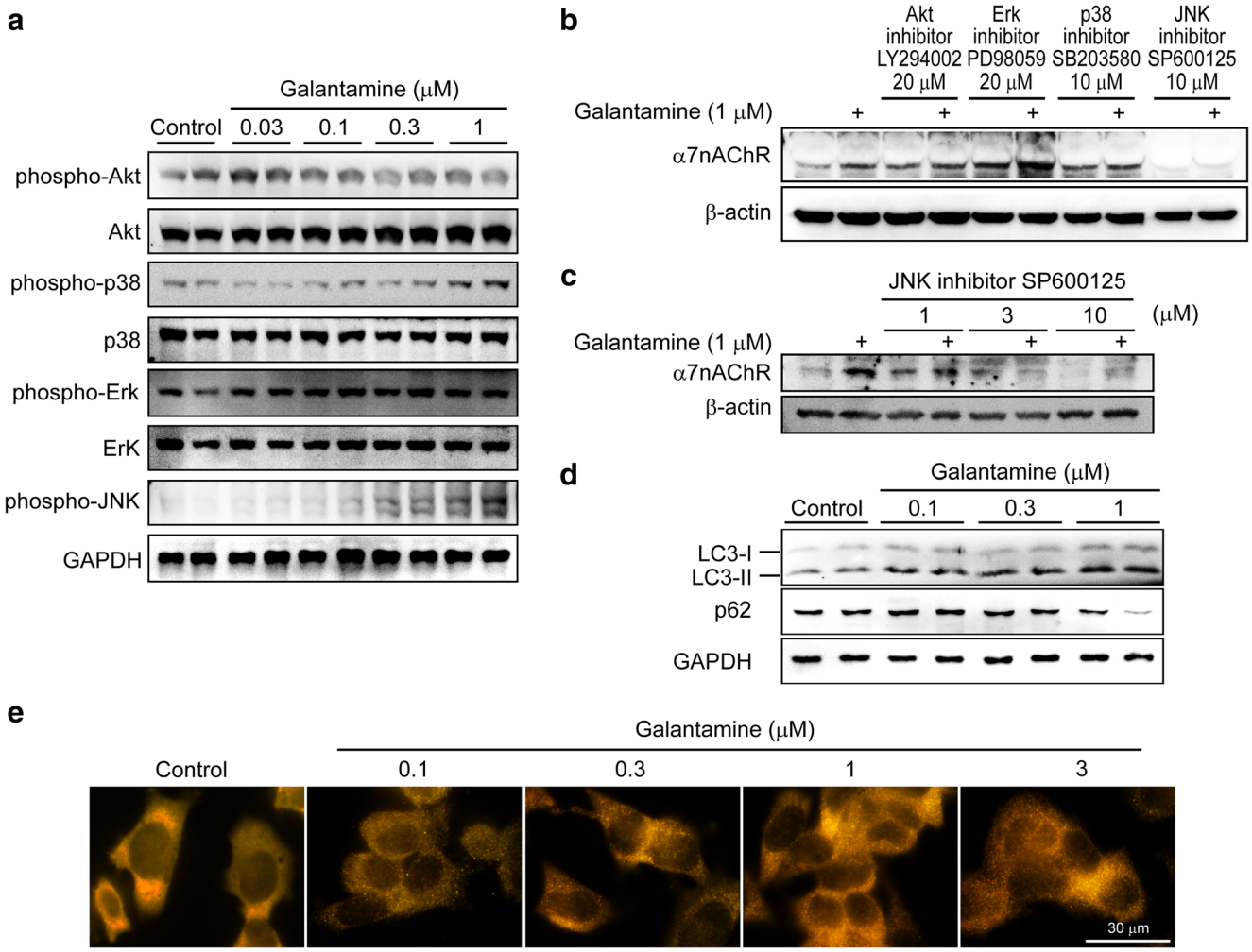

Fig. 2 Galantamine activates the MAPK/JNK signaling pathway to enhance α7nAChR expression and inhibits the PI3K/Akt signaling pathway to activate autophagy in neurons. (a) Western blot results show that treatment with galantamine (0.03-1 μM) for 4 h dose-dependently suppressed Akt, increased p38 and JNK, but did not affect Erk phosphorylation in SH-SY5Y cells. (b) Western blot data show that galantamine treatment for 24 h induced α7nAChR upregulation in SH-SY5Y cells as compared to no-treatment control. The MAPK/JNK signaling pathway inhibitor SP600125 (10 μM) antagonized galantamine-induced α7nAChR upregulation, whereas no such effect was seen with the PI3K/Akt inhibitor LY294002 (20 μM), the MAPK/Erk inhibitor PD98059 (20 μM), or the MAPK/p38 inhibitor SB203580 (10 μM). (c) Cells were treated with 1 to 10 μM JNK inhibitor for 24 h; Western blot data show that 10 μM but not 1 or 3 μM JNK inhibitor SP600125 completely abolished the endogenous α7nAChR expression as compared to no-treatment control; 10 μM (but not 1 or 3 μM) JNK inhibitor SP600125 co-treatment with galantamine inhibited galantamine-induced α7nAChR expression. (d) LC3-II and p62 are associated with autophagosome formation (LC3-II↑ when autophagosome↑) and autophagic flux (p62↓ when cargo degradation↑), respectively. Western blot results show that treating SH-SY5Y cells with galantamine (0.1-1 μM) for 4 h dose-dependently increased autophagosome formation (LC3-II↑) and autophagic flux (p62↓). (e) Immunofluorescent staining of LC3 shows that treating cells with galantamine for 4 h dose-dependently increased autophagosome formation, as demonstrated by the fluorescent punctate dots of LC3-II in the SH-SY5Y cells

induced α7nAChR expression 24 h after cells were treated with 1 μM galantamine (Fig. 2b). We then treated cells with 1 to 10 μM JNK inhibitor for 24 h; the result shows 10 μM but not 1 or 3 μM JNK inhibitor SP600125 completely abolished the endogenous α7nAChR expression (Fig. 2c). Galantamine (1 μM) enhanced α7nAChR expression; 10 μM (but not 1 or 3 μM) JNK inhibitor SP600125 cotreatment with galantamine completely inhibited galantamine-induced α7nAChR expression (Fig. 2c). The result is consistent with Fig. 2b, indicating that galantamine increases α7nAChR expression by activating the MAPK/JNK signaling pathway. The PI3K/Akt/mTOR pathway serves as the primary autophagy regulatory pathway and Akt inhibition promotes autophagy [26]. Figure 2a shows that galantamine treatment inhibited Akt phosphorylation. We then tested the effects of galantamine in autophagy activation. LC3 and p62 are widely accepted as markers of autophagosomes and autophagic flux, respectively. The conversion of LC3-I into LC3-II (LC3 lipidation) is indicative of autophagic activity; the amount of LC3-II correlates well with the number of autophagosomes. Western blot results show that galantamine (0.1-1 μM) treatment of SH-SY5Y cells for 4 h dose-dependently increased autophagosome formation (LC3-II↑) and autophagic flux (when p62↓) (Fig. 2d). Immunofluorescence staining of LC3 shows that SH-SY5Y cells treated with galantamine (0.1-3 μM) for 4 h dose-dependently increased autophagosome formation, as demonstrated by the fluorescent punctate dots of LC3-II in the cytoplasm (Fig. 2e), which suggests that galantamine activates autophagy and enhances autophagy flux in neurons.

Galantamine Regulates Autophagosome Biogenesis and Enhances Neuroprotective Protein Expression in Neurons

Autophagosome biogenesis contains several steps, including phagophore induction (nucleation), phagophore elongation, and autophagosome formation [27]. Beclin 1 is a critical regulator in the autophagic initiation process, which involves nucleation of the phagophore [28]. Interactions between Beclin 1 and class III phosphatidylinositol 3-kinase (PI3KC3)/VPS34, Ambra1, Vps15, and Atg14L lead to autophagy activation [28]. The conversion of LC3-I to LC3-II is mediated by Atg3, Atg5, and Atg7 [27]. We found galantamine dose-dependently enhanced the expressions of Beclin 1, Atg3 (an essential protein for autophagosome formation) and autophagy proteins Atg5, Atg7, and Atg9A (mediators of phagophore elongation) in SH-SY5Y cells 4 h after galantamine treatment (Fig. 3a). PTEN-induced putative kinase 1 (PINK1) is a mitochondrial serine/threonine–protein kinase that can protect cells from stress-induced mitochondrial dysfunction, whereas DJ-1 is an antioxidant protein that regulates mitochondrial function and autophagy; both mediate mitophagy [29–31]. We found that treating SH-SY5Y cells

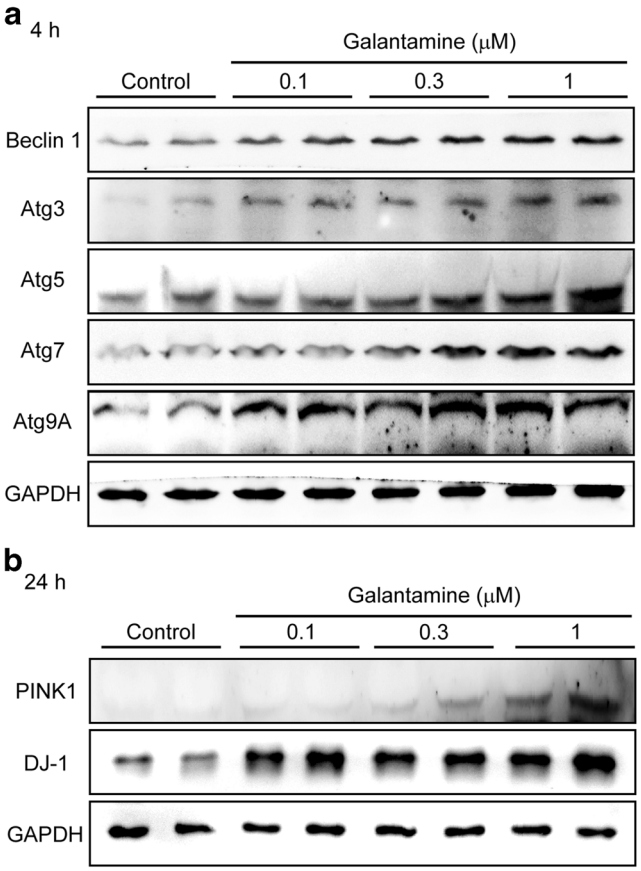

Fig. 3 Galantamine enhances autophagy, autophagosome biogenesis, and mitophagy in neurons. Beclin 1 is an autophagy inductor; Atg3, Atg5, Atg7, and Atg9A are involved in autophagosome biogenesis. (a) Expressions of Beclin 1 and autophagosome formation proteins Atg3, Atg5, and Atg7 in SH-SY5Y cells were increased after treatment with galantamine for 4 h. (b) PINK1 and DJ-1 regulate mitochondrial function and promote mitophagy. After SH-SY5Y cells were treated with galantamine (0.1-1 μM) for 24 h, Western blot results show that galantamine dose-dependently enhanced PINK1 and DJ-1 expressions

with galantamine for 24 h dose-dependently enhanced PINK1 and DJ-1 expression (Fig. 3b). It is known that full-length PINK1 interacts with Beclin 1 and that the accumulation of PINK1 expression promotes autophagy [32]. In line with these findings, our data indicate that galantamine modulates the process of autophagosome biogenesis and might also regulate mitophagy by clearing away dysfunctional mitochondria and protect against neuronal apoptosis.

α7nAChR Involvement in the Neuroprotective Ability of Galantamine Against $A\beta_{1-42}$-Induced Neurotoxicity

We pretreated SH-SY5Y cells with the α7nAChR-specific antagonist MLA (10 nM) for 30 min to block the function of α7nAChR-mediated signaling, before applying $A\beta_{1-42}$ (30 μM) for 48 h. Hoechst staining results revealed that galantamine (1 μM), MLA (10 nM), or galantamine + MLA did not cause cell apoptosis as compared to no-treatment control

(Fig. 4a). $A\beta_{1–42}$ (30 μM) enhanced cell apoptosis in SH-SY5Y cells (Fig. 4a). Arrows indicate the nuclear condensation cells, shown as magnified images in the upper right-hand corner of each lower panel. With $A\beta_{1–42}$ treatment, galantamine (1 μM) but not MLA cotreatment with $A\beta_{1–42}$ inhibited $A\beta_{1–42}$-induced apoptosis; MLA antagonized galantamine-induced neuroprotection against $A\beta_{1–42}$ neurotoxicity in the galantamine + MLA group (Fig. 4a). The right panel of Fig. 4a is the summarized data of the Hoechst staining. Western blot results show that whereas $A\beta_{1–42}$ promoted PARP cleavage and Bax expression, both were reduced by galantamine (Fig. 4b). MLA pretreatment abolished galantamine-induced neuroprotection against $A\beta_{1–42}$ neurotoxicity (cleaved PARP↑ and Bax↑ in the galantamine + MLA group; Fig. 4b). Right panels of Fig. 4b show the summarized results of PARP, cleaved PARP, and Bax expressions. Since MLA treatment abolished galantamine-induced neuroprotection against $A\beta_{1–42}$ neurotoxicity, we then used pLKO1-shα7nAChR-A or

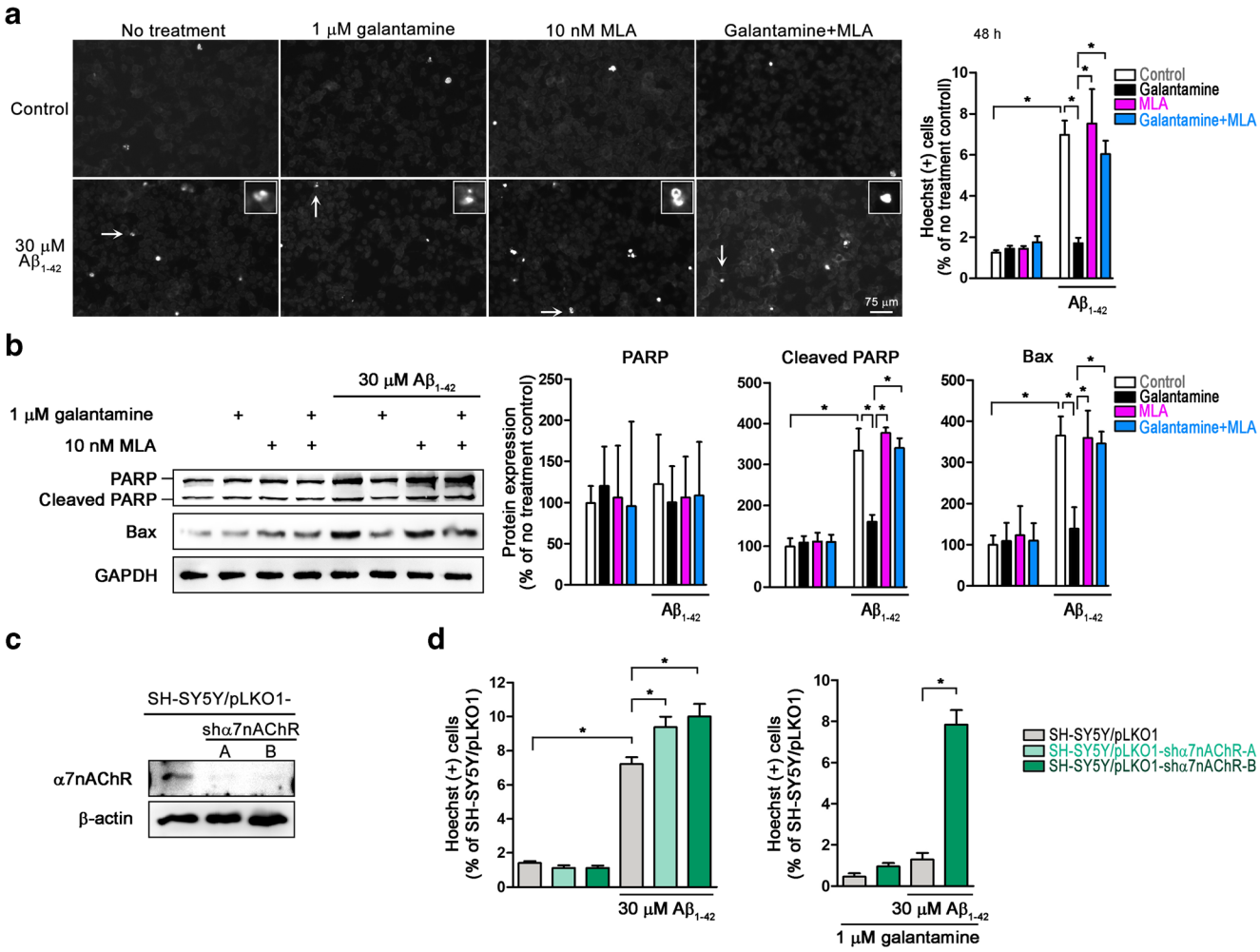

Fig. 4 α7nAChR involvement in the neuroprotective effects of galantamine against $A\beta_{1–42}$ neurotoxicity. (a) Hoechst staining reveals $A\beta_{1–42}$ (30 μM)-induced neuronal apoptosis in SH-SY5Y cells at 48 h after treatment. Galantamine (1 μM) reduced $A\beta_{1–42}$-induced apoptosis. Using the α7nAChR antagonist MLA (10 nM) to block the function of α7nAChR, MLA co-treatment with galantamine antagonized galantamine-induced neuroprotection against $A\beta_{1–42}$ neurotoxicity. Arrows indicate the nuclear condensation cells, shown as magnified images in the upper right-hand corner of each lower panel. Summarized results from Hoechst staining are depicted in the bar graph. (b) Cleavage of PARP by caspases and increased Bax expression are hallmarks of apoptotic cell death. Western blot results show that $A\beta_{1–42}$ treatment for 48 h enhanced PARP cleavage and Bax expression in SH-SY5Y cells. Compared to $A\beta_{1–42}$, galantamine (1 μM) treatment for 48 h reduced $A\beta_{1–42}$-induced PARP cleavage and Bax expression. MLA co-treatment with galantamine antagonized the effects of galantamine, as shown by an increase in $A\beta_{1–42}$-induced PARP cleavage and Bax expression. Summarized results of PARP, cleaved PARP, and Bax expressions are depicted in the bar graph; (c) Western blot results of α7nAChR knockdown efficacy of pLKO1-shα7nAChR-A or pLKO1-shα7nAChR-B plasmid at 72 h after transfection to SH-SY5Y. In this study, pLKO1 plasmid was used as a negative control. (d) Hoechst staining revealed that cells transfected with pLKO1-shα7nAChR-A or pLKO1-shα7nAChR-B to knockdown endogenous α7nAChR significantly enhanced $A\beta_{1–42}$-induced neurotoxicity at 48 h after treatment as compared to pLKO1 control. In α7nAChR knockdown cells (SH-SY5Y/pLKO1-shα7nAChR-B), galantamine (1 μM) lost the neuroprotection against $A\beta_{1–42}$ neurotoxicity as compared to SH-SY5Y/pLKO1 control cells. Data are expressed as mean ± SEM. $^*p < 0.05$

pLKO1-shα7nAChR-B plasmid to knockdown endogenous α7nAChR expression in SH-SY5Y. Figure 5c shows the α7nAChR knockdown efficacy of pLKO1-shα7nAChR-A or pLKO1-shα7nAChR-B plasmid 72 h after transfection. This study used pLKO1 plasmid as negative control. Hoechst staining results revealed that using pLKO1-shα7nAChR-A or pLKO1-shα7nAChR-B to knockdown α7nAChR significantly enhanced $A\beta_{1-42}$-induced neurotoxicity 48 h after $A\beta_{1-42}$ treatment as compared to the pLKO1 control (Fig. 4d). In α7nAChR knockdown cells (SH-SY5Y/pLKO1-shα7nAChR-B), galantamine (1 μM) lost the neuroprotection against $A\beta_{1-42}$ neurotoxicity as compared to SH-SY5Y/pLKO1 control that is consistent with our MLA data (Fig. 4d), suggesting that the neuroprotective ability of galantamine against $A\beta_{1-42}$ neurotoxicity is associated with α7nAChR.

α7nAChR Enhances Autophagy, Autophagosome Biogenesis, and Mitophagy Against $A\beta_{1-42}$ Neurotoxicity

Since galantamine-induced neuroprotection and autophagic induction were associated with α7nAChR expression, we then sought to determine whether α7nAChR overexpression is consistent with galantamine treatment. Figure 5a illustrates the plasmid construction of the pCDNA3.1-α7nAChR vector, which we used to generate α7nAChRs stably expressing cell clones in SH-SY5Y cells. Western blot results revealed increased α7nAChR expression in 3 α7nAChR stable cell clones, SH-SY5Y/pCDNA3.1-α7nAChR-C4, SH-SY5Y/pCDNA3.1-α7nAChR-C5, and SH-SY5Y/pCDNA3.1-α7nAChR-C6, as compared to 2 control cell clones, SH-SY5Y/pCDNA3.1-His-C1 and SH-SY5Y/pCDNA3.1-His-C2 (Fig. 5b). α7nAChR overexpression

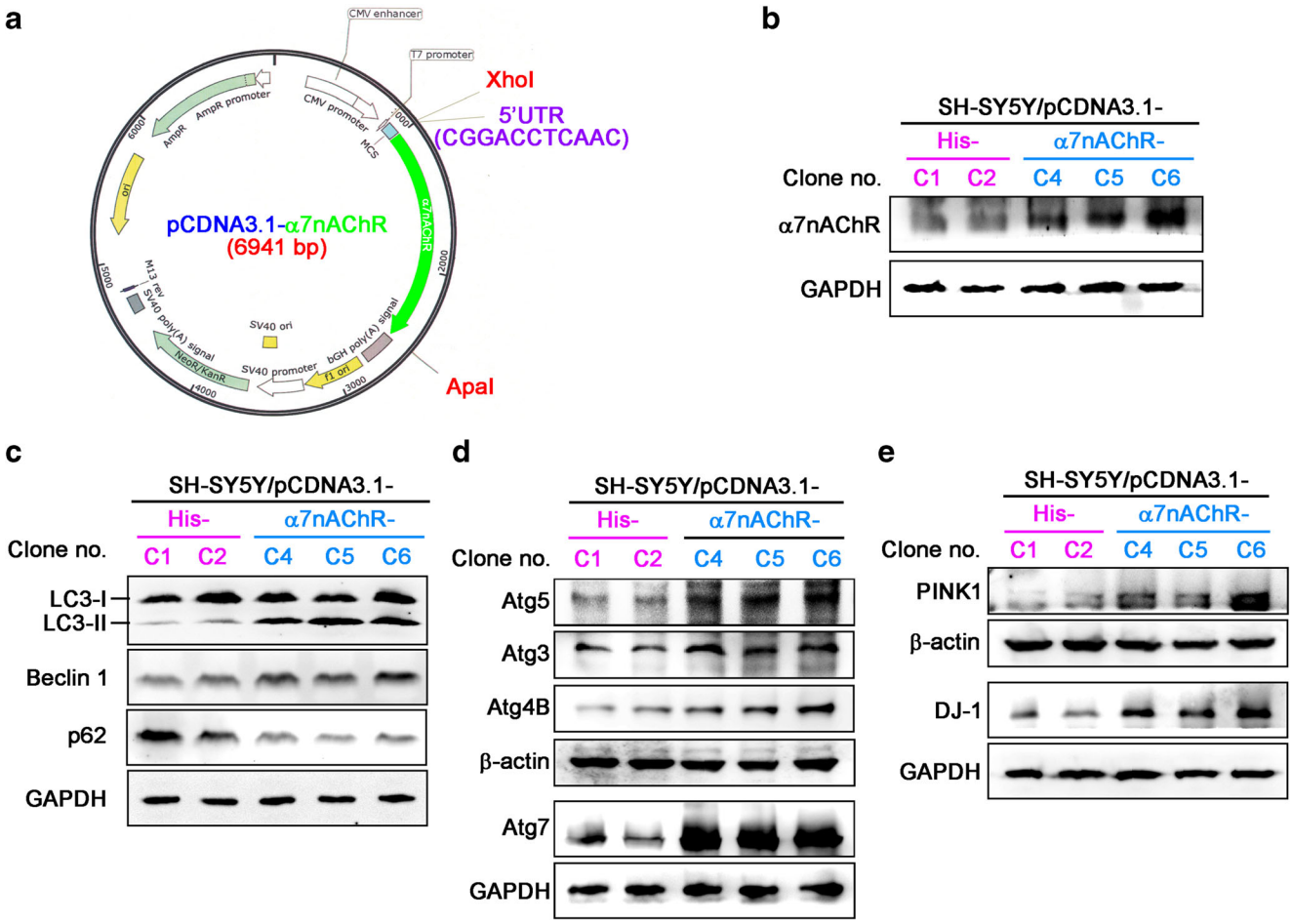

Fig. 5 α7nAChR overexpression enhances autophagy, autophagosome biogenesis, and mitophagy in neurons. (a) Diagram of the pCDNA3.1-α7nAChR expression vector, which was used to generate α7nAChR stably expressing cell clones that were transfected into SH-SY5Y cells. (b) Western blot results show increases in α7nAChR expression in 3 α7nAChR stable cell clones, SH-SY5Y/pCDNA3.1-α7nAChR-C4, SH-SY5Y/pCDNA3.1-α7nAChR-C5, and SH-SY5Y/pCDNA3.1-α7nAChR-C6, as compared to 2 control cell clones, SH-SY5Y/pCDNA3.1-His-C1 and SH-SY5Y/pCDNA3.1-His-C2. (c) α7nAChR overexpression increased autophagosome formation (Beclin 1↑ and LC3-II↑) and autophagic flux (p62↓) in 3 α7nAChR stably expressing cell clones but not in the 2 control cell clones. (d) α7nAChR overexpression enhanced the expression of Ag5, Atg3, Atg4B, and Atg7, each of which regulates autophagosome biogenesis. (e) α7nAChR overexpression enhances the expression of PINK1 and DJ-1, which both promote mitophagy.

enhanced autophagosome formation (Beclin 1↑ and LC3-II↑) and autophagic flux (p62↓) in the α7nAChR cell clones but not the control cell clones (Fig. 5c). α7nAChR overexpression also enhanced the expression of Atg3, Atg4B, Atg5, and Atg7, all of which are involved in autophagosome biogenesis, and increased the expression of PINK1 and DJ-1, which activate mitophagy (Fig. 5d, e). Hoechst staining revealed that α7nAChR overexpression (SH-SY5Y/pCDNA3.1-α7nAChR-

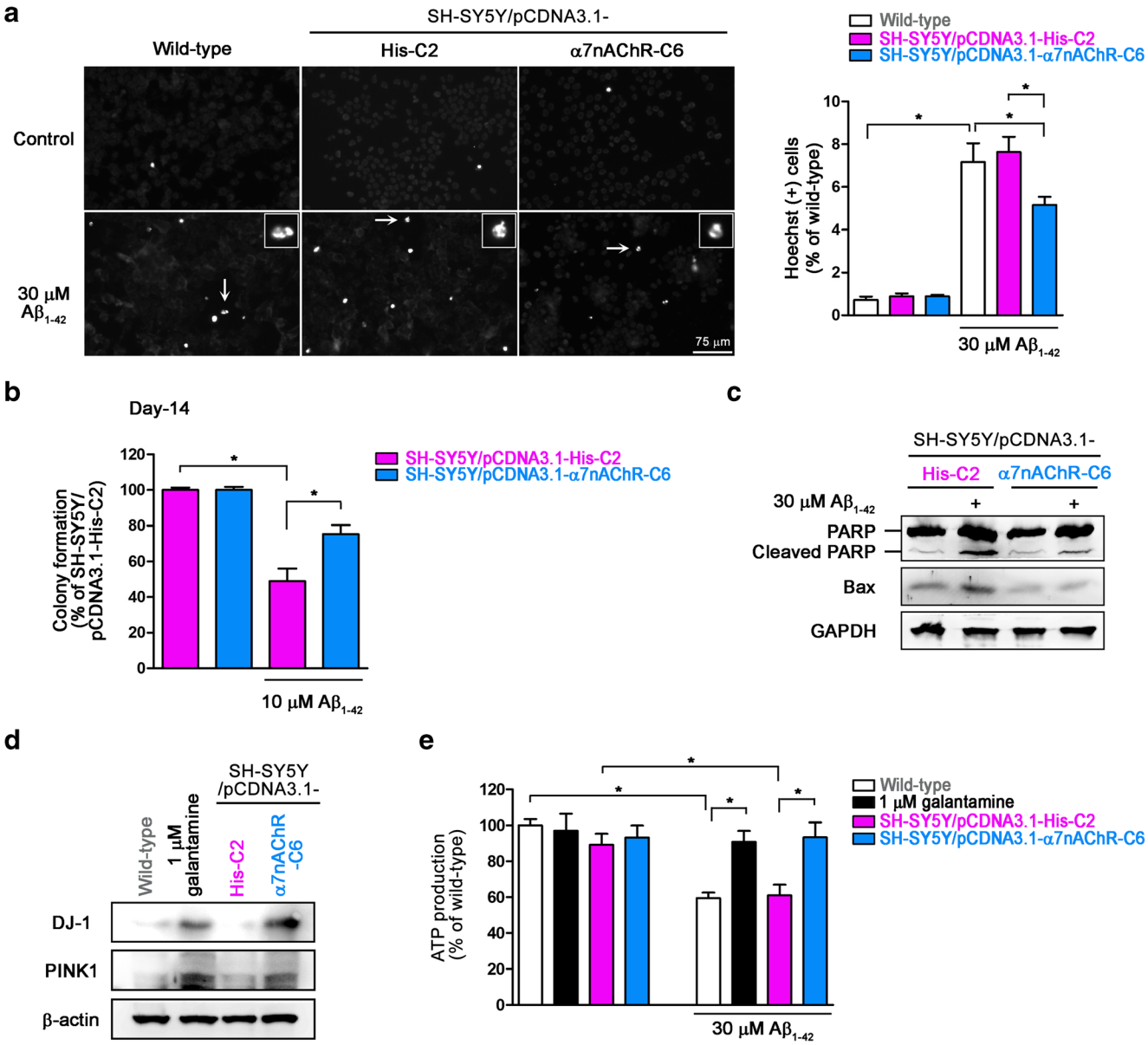

Fig. 6 α7nAChR overexpression suppresses $A\beta_{1-42}$ neurotoxicity in SH-SY5Y cells. (a) After 48 h of $A\beta_{1-42}$ (30 μM) treatment, Hoechst staining revealed that α7nAChR-overexpressing cells (SH-SY5Y/pCDNA3.1-α7nAChR-C6) reduced apoptosis which induced by $A\beta_{1-42}$ as compared to the wild-type cells and SH-SY5Y/pCDNA3.1-His-C2 control clone. Arrows indicate nuclear condensation cells, shown as magnified images in the upper right-hand corner of each panel. Summarized results of Hoechst staining are shown in the right bar graph. (b) The colony formation assay measured cell proliferation after 14 days of treatment with $A\beta_{1-42}$ (10 μM). α7nAChR-overexpressing cells (SH-SY5Y/pCDNA3.1-α7nAChR-C6) increased colony formation as compared to SH-SY5Y/pCDNA3.1-His-C2 cells. (c) Western blot results show that 48 h of treatment with $A\beta_{1-42}$ (30 μM) enhanced PARP cleavage and Bax expression in SH-SY5Y/pCDNA3.1-His-C2 cells. Compared to SH-SY5Y/pCDNA3.1-His-C2 cells, α7nAChR-overexpressing cells (SH-SY5Y/pCDNA3.1-α7nAChR-C6) reduced $A\beta_{1-42}$-induced PARP cleavage and Bax expression. (d) Mitophagy selectively degrades mitochondria by autophagy. PINK1 and DJ-1 regulate mitophagy. Western blot results show that galantamine treatment for 24 h or α7nAChR overexpression (SH-SY5Y/pCDNA3.1-α7nAChR-C6) enhanced DJ-1 and PINK1 expressions as compared to wild type or SH-SY5Y/pCDNA3.1-His-C2, respectively. (e) $A\beta_{1-42}$ (30 μM) treatment for 48 h significantly reduced mitochondrial ATP production in wild-type SH-SY5Y cells. Galantamine (1 μM) treatment or α7nAChR overexpression (SH-SY5Y/pCDNA3.1-α7nAChR-C6) rescued $A\beta_{1-42}$-induced ATP reduction as compared to wild type or SH-SY5Y/pCDNA3.1-His-C2, respectively. Data are expressed as mean ± SEM. $^*p < 0.05$

C6 clone) reduced $A\beta_{1-42}$-induced apoptosis as compared to the wild-type control and SH-SY5Y/pCDNA3.1-His-C2 clone (Fig. 6a). Arrows indicate nuclear condensation cells, shown as magnified images in the upper right-hand corner of each lower panel. Using the colony formation assay to measure cell proliferative capacity under $A\beta_{1-42}$-induced neurotoxicity, we found that α7nAChR overexpression (SH-SY5Y/pCDNA3.1-α7nAChR-C6) enhances colony formation as compared to SH-SY5Y/pCDNA3.1-His-C2 (Fig. 6b). Increases in PARP cleavage and Bax expression are associated with cell apoptosis. Western blot results revealed that $A\beta_{1-42}$ enhanced PARP cleavage and Bax expression in the SH-SY5Y/pCDNA3.1-His-C2 clone, whereas α7nAChR overexpression by the SH-SY5Y/pCDNA3.1-α7nAChR-C6 clone reduced $A\beta_{1-42}$-induced PARP cleavage and Bax expression (Fig. 6c). Mitophagy selectively degrades mitochondria by autophagy. PINK1 and DJ-1 both regulate mitophagy. Figure 6d shows galantamine (1 μM) treatment for 24 h or α7nAChR overexpression (SH-SY5Y/pCDNA3.1-a7nAChR-C6) enhanced DJ-1 and PINK1 expressions as compared to wild-type SH-SY5Y or SH-SY5Y/pCDNA3.1-His-C2, respectively. $A\beta_{1-42}$ (30 μM) treatment for 48 h significantly reduced mitochondrial ATP production in wild-type SH-SY5Y (Fig. 6e). Galantamine (1 μM) treatment or α7nAChR overexpression (SH-SY5Y/pCDNA3.1-α7nAChR-C6) rescued $A\beta_{1-42}$-induced ATP reduction as compared to wild type or SH-SY5Y/pCDNA3.1-His-C2, respectively (Fig. 6e). These results indicate that α7nAChR overexpression enhances autophagy, autophagosome

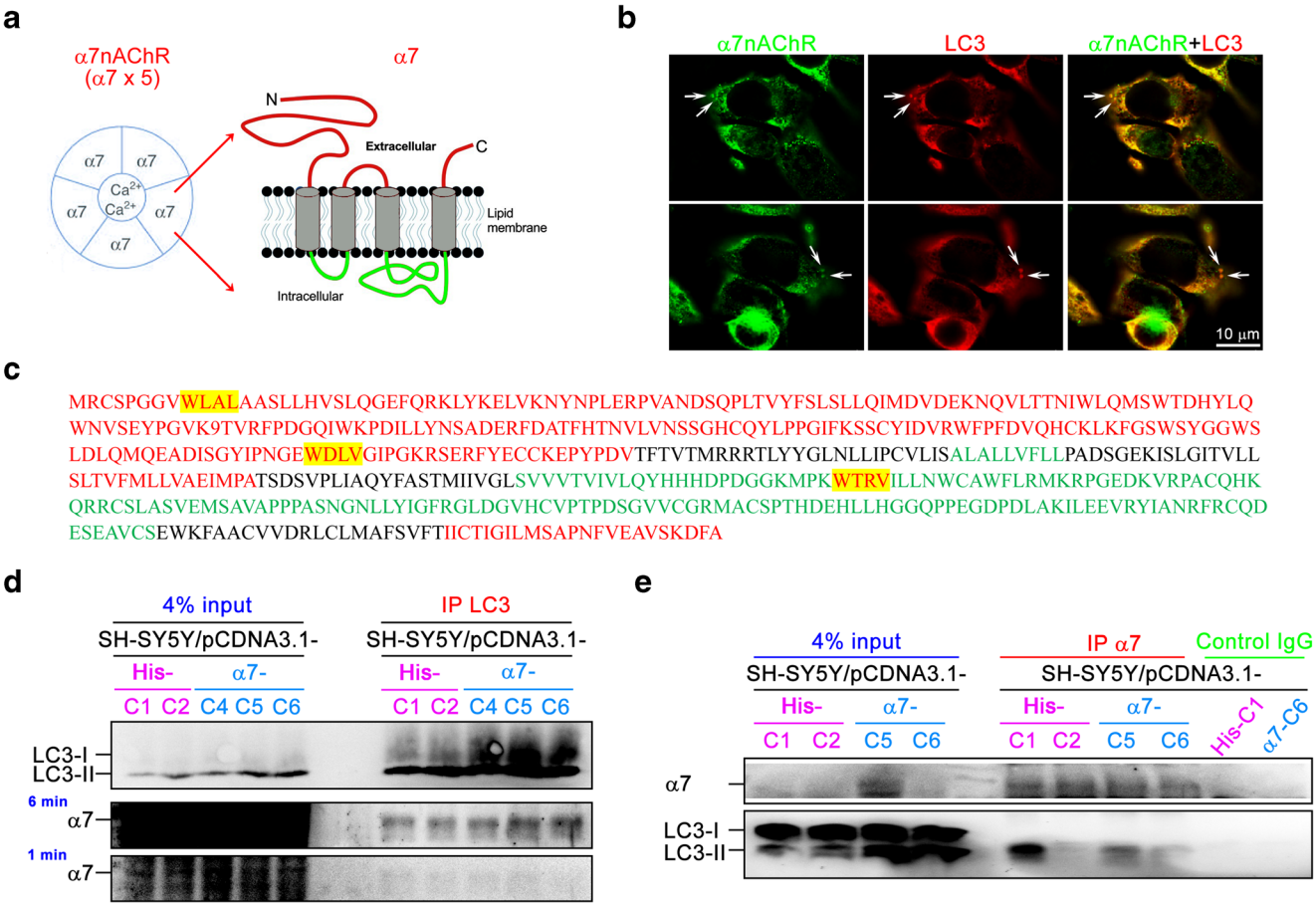

Fig. 7 α7nAChR acts as a cargo carrier for autophagosomal marker protein LC3 binding during autophagy. Specific cargo carriers (receptors) are responsible for selective autophagy, tethering the cargo to the site of autophagosomal engulfment by binding with LC3. (a) α7nAChR is Ca^{2+}-permeable and contains 5 α7 subunits; α7 is a transmembrane protein with extracellular (red), transmembrane (gray), and intracellular (green) domains. (b) Confocal images of immunodouble staining show that α7nAChR colocalized with LC3-II in α7nAChR overexpression cells (SH-SY5Y/pCDNA3.1-α7nAChR-C6). Arrows indicate sites of α7nAChR and LC3-II colocalization. (c)The protein sequence of α7 contains 3 possible LC3-interacting regions, each of which is highlighted in yellow. The extracellular, transmembrane, and intracellular domains of α7 discussed in the text are depicted in red, black, and green, respectively. (d) Using an antibody to immunoprecipitate LC3 (IP LC3) shows that the anti-LC3 antibody was effectively immunoprecipitated LC3 in each stably expressing clone as compared to 4% input (lysate). Western blot results of 3 α7nAChR stably expressing clones (α7nAChR-C4, α7nAChR-C5, and α7nAChR-C6) show that α7nAChR overexpression enhanced LC3 binding with α7 in SH-SY5Y cells; 6 min and 1 min represent the image exposure times of α7 expression. (e) Using an antibody to immunoprecipitate α7 (IP α7) shows that α7 binds with LC3-II in all cell clones. This study used rabbit IgG isotype control (control IgG) as a negative control

biogenesis, and mitophagy against $A\beta_{1–42}$ neurotoxicity, which is consistent with galantamine treatment.

α7nAChR Binds with the Autophagosomal Marker Protein LC3 as a Cargo Carrier in Autophagy

Cargo carriers (receptors, e.g., p62, NBR1) are responsible for selective autophagy which contain LC3-interacting region for tethering cargo to the site of autophagosomal engulfment by binding with the autophagosomal marker protein LC3 [33]. α7nAChR is composed of 5 α7 subunits, each of which contains 4 hydrophobic transmembrane regions [15]. Figure 7a shows the extracellular, transmembrane, and intracellular domains of the α7 subunit in red, gray, and green, respectively. Confocal images of immunodouble staining show that α7nAChR colocalized with LC3-II (autophagosomes) in α7nAChR overexpression cells (SH-SY5Y/pCDNA3.1-α7nAChR-C6). Arrows indicate sites of α7nAChR and LC3-II colocalization (Fig. 7b). We found that the protein sequence of α7 has 3 LC3-interacting regions—WLAL, WDLV, and WTRV—each of which is highlighted in yellow in Fig. 7c, whereas sequences of the extracellular, transmembrane and intracellular domains of the α7 protein are shown in red, black, and green, respectively. Since α7 contains LC3-interacting regions that may bind with LC3, we then used an antibody to immunoprecipitate LC3 or α7 protein (IP LC3 or α7). Figure 7 d and e show that both the anti-LC3 and anti-α7 antibodies very effectively immunoprecipitated LC3 or α7 protein as compared to 4% input (lysate). Western blot results of 3 α7nAChR stably expressing clones (α7nAChR-C4, α7nAChR-C5, and α7nAChR-C6) show that α7nAChR overexpression enhanced LC3 binding with α7 in SH-SY5Y cells (6 min and 1 min indicate the image exposure time of α7; Fig. 7d). In α7 IP, we found that α7 binds with LC3-II in all clones (control IgG was used as the negative control; Fig. 7e). These data suggest that α7nAChR acts as a cargo carrier for autophagosomal marker-LC3 binding during autophagy.

Discussion

The neuroprotective effect from α7nAChR agonists such as nicotine may be through α7nAChR upregulation and then desensitization/inactivation, but not activation [34]. Our previous studies have shown that extracellular $A\beta_{1–42}$ binding with α7nAChR is an important step in Aβ detoxification that further enhances the autophagic activity for Aβ clearance [12, 13]. The α7nAChR-overexpressing neuroblastoma-SK-N-MC cells exhibited rapid binding, internalization, and accumulation of exogenous $A\beta_{1–42}$, but not $A\beta_{1–40}$; the importance of this process is emphasized by the fact that this internalization was blocked by the α7nAChR antagonist-α-bungarotoxin and endocytosis inhibitor-phenylarsine oxide [17]. In this study, we found galantamine against $A\beta_{1–42}$-induced neuronal apoptosis via enhancing α7nAChR expression, autophagy, autophagosome biogenesis, and mitophagy. By manipulating α7nAChR expression, we found that α7nAChR enhances autophagy, autophagosome biogenesis, and mitophagy against $A\beta_{1–42}$ neurotoxicity, all of which is consistent with galantamine in Aβ detoxification. After cell surface α7nAChR binding with extracellular $A\beta_{1–42}$ (cargo), α7nAChR is desensitized and the Aβ-α7nAChR complex is internalized into the cytoplasm by endocytosis. The novelty of our study finding is the discovery that α7 contains 3 LC3-interacting regions and acts as a cargo carrier to bind with the autophagosomal marker protein LC3 and thus tether the cargo–cargo carrier complex $A\beta_{1–42}$-α7nAChR into the autophagosome. Our study suggests that the neuroprotective effect of galantamine against $A\beta_{1–42}$ neurotoxicity occurs via the upregulation of α7nAChR expression and α7nAChR is the key mediator for Aβ clearance in neurons by selective autophagy. Figure 8 illustrates our proposed model of how

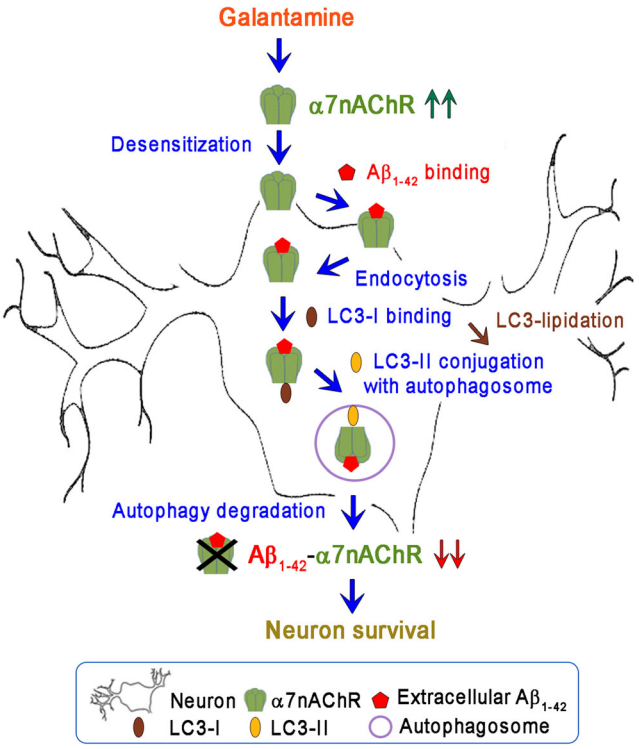

Fig. 8 Our proposed model showing how galantamine protects against $A\beta_{1–42}$-induced neurotoxicity and the role played by α7nAChR in galantamine-induced neuroprotection during selective autophagy of $A\beta_{1–42}$. Galantamine upregulates α7nAChR expression and then desensitizes α7nAChR. After α7nAChR binds with extracellular $A\beta_{1–42}$, the $A\beta_{1–42}$–α7nAChR complex on the cell surface enters into the cytoplasm by endocytosis, in which α7nAChR acts as a cargo carrier for binding of the autophagosomal marker protein LC3. In selective autophagy for $A\beta_{1–42}$ clearance, α7nAChR binding with LC3 is an important step for the engulfment of the cargo ($A\beta_{1–42}$) and the cargo carrier (α7nAChR) to autophagosomes and then degradation $A\beta_{1–42}$–α7nAChR complexes by autophagy

galantamine acts against $A\beta_{1-42}$ neurotoxicity and the role of α7nAChR in galantamine-induced neuroprotection during autophagy.

α7nAChRs have been shown to modulate neuron excitability, neurotransmitter release, the induction of LTP, learning, and memory, and are particularly enriched in cholinergic target areas of the brain [35, 36]. The PI3K/Akt signaling pathway is a well-known autophagy regulation pathway, and previous studies indicated the JNK signaling pathway also controls autophagy through regulating expressions of autophagy-related genes [37]. The regulatory mechanism of α7nAChR expression is unclear; only 1 study shows the AP-2α (a transcription factor of AP-2 family) negatively regulates α7nAChR expression in SH-SY5Y cells [38]. Our result shows that 1) galantamine activated the JNK signaling pathway, 2) blocking the JNK signaling pathway abolishes endogenous and galantamine-induced α7nAChR expression, and 3) autophagy regulates α7nAChR degradation in SH-SY5Y. Further research is needed to determine the relationship of the JNK signaling pathway and α7nAChR expression. α7nAChRs and $A\beta_{1-42}$ interact with high affinity; initial Aβ deposition in early AD overlaps with α7nAChR expression in the basal forebrain cholinergic system, including the hippocampus [35, 38]. Exposure to $A\beta_{1-42}$ results in rapid depletion of cell surface-associated α7nAChRs and redistribution of α7nAChRs to intracellular $A\beta_{1-42}$-positive deposits; this process is also assisted by treatment with a nicotinic agonist, which can induce α7nAChR internalization without $A\beta_{1-42}$ [17]. In this study, we found that galantamine against $A\beta_{1-42}$-induced neurotoxicity via activating the MAPK/JNK and inhibiting PI3K/Akt signaling pathways to enhance α7nAChR expression and autophagy, respectively. An Aβ-α7nAChR interaction under "high Aβ" amyloid conditions can result in 1) perturbation and dysregulation of signal transduction mechanisms involved in synaptic plasticity and homeostasis; 2) internalization of the Aβ-receptor complex; 3) cell toxicity; and 4) amyloid plaque seeding [35]. α7nAChRs mediate neuroprotective effects of nicotine against Aβ toxicity via the PI3K/Akt pathway in cultured neurons [39]. Protection against Aβ toxicity is proportional to the number of α7nAChRs expressed by cultured cells [34], which indicates that α7nAChR is required for intracellular $A\beta_{1-42}$ accumulation and internalization of the $A\beta_{1-42}$-α7nAChR complex occurring via endocytosis in neurons.

Amino acid residues of the LC3-interacting region are evolutionarily conserved in the W/F/Y-X-X-L/I/V logo sequence of the cargo carrier (receptor) [33]. In our study, we have found that the protein sequence of α7 contains 3 possible LC3-interacting regions, namely WLAL and WDLV in the extracellular domain and WTRV in the intracellular domain of α7. We also observed that α7 binds with the autophagosomal marker protein LC3, indicating that α7nAChR acts as a cargo carrier for $A\beta_{1-42}$ (cargo) and autophagosomal marker protein-LC3 binding. This is the first report to provide evidence of the cell surface receptor α7nAChR acting as a cargo carrier for LC3 binding in the cytoplasm during selective autophagy of $A\beta_{1-42}$ clearance. Further research is needed to determine the precise binding/interaction site between α7 and LC3.

Autophagy declines with AD progression, contributing to Aβ deposition [40]. In AD, autophagosome biogenesis is impaired, and Aβ-containing autophagosomes consequently accumulate [41]. Approximately 35 genes participate in autophagy (the so-called autophagy-related genes), regulating autophagosome biogenesis in phagophore induction (nucleation), phagophore elongation, and autophagosome formation [42]. In this study, we found that galantamine activates autophagy by enhancing phagophore induction (Beclin 1↑), phagophore elongation (Atg5↑, Atg7↑, and Atg9A↑), and autophagosome formation (Atg3↑ and LC3-II↑) in neurons. Our data also show that α7nAChR overexpression affects the same steps in phagophore induction (Beclin 1↑), phagophore elongation (Atg5↑ and Atg7↑), and autophagosome formation (Atg3↑, Atg4B↑, and LC3-II↑) in 3 α7nAChR cell clones, each of which expressed different levels of α7nAChR. Beclin 1 reduces expression in early AD; Beclin 1 deficiency disrupts neuronal autophagy and promotes Aβ accumulation and neurodegeneration in mice [43], which suggests that α7nAChR is the key molecular mechanism in galantamine-induced autophagy.

Mitochondrial dysfunction contributes to AD; maintenance of mitochondrial health depends on mitochondrial biogenesis and the efficient clearance of dysfunctional mitochondria through mitophagy to prevent mitochondria-induced cellular dysfunction [44]. In this study, we found that galantamine or α7nAChR overexpression enhanced PINK1 and DJ-1 expressions and abolished $A\beta_{1-42}$-induced ATP reduction in neurons. In HeLa cells, PINK1 recruits autophagy receptors to induce low-level mitophagy in a Parkin-independent manner [45]. DJ-1 overexpression induces Erk-dependent mitophagy and protects against rotenone-induced apoptosis [31]; loss of DJ-1 leads to mitochondrial phenotypes including reduced membrane potential and increased fragmentation [46]. All of these data indicate that galantamine- or α7nAChR-induced activation of mitophagy may be useful in AD.

Autophagy induction can be beneficial as a disease-modifying treatment in experimental models of various neurodegenerative diseases [11]. A better understanding of these mechanisms will provide a good rationale for the design of novel therapies for neurodegenerative disease. Our study data elucidate new, favorable therapeutic aspects of galantamine for people diagnosed with AD.

Acknowledgments This work was supported by grants from the Ministry of Science and Technology of Taiwan (MOST 108-2320-B-039-029-MY3) and China Medical University Hospital (DM-105-084), and partly supported by the integrative Evolutionary Galliform Genomics (iEGG) and Animal Biotechnology Center in The Feature Areas Research Center Program within the framework of the Higher Education Sprout Project led by the Ministry of Education (MOE-107-S-0023-E). We thank Iona J. MacDonald from China Medical University for her editing of this paper.

Compliance with Ethical Standards

Conflict of Interest The authors declare that they have no conflict of interest.

References

1. Dementia fact sheet. World Health Organization. 2017.
2. Alzheimer's A. 2013 Alzheimer's disease facts and figures. Alzheimers Dement. 2013;9(2):208–45.
3. Prince MA, E.; Guerchet, M.; Prina M. World Alzheimer report 2014: dementia and risk reduction. an analysis of protective and modifiable risk factors. London: Alzheimer Disease International. 2014.
4. Dubois B, Feldman HH, Jacova C, Hampel H, Molinuevo JL, Blennow K, et al. Advancing research diagnostic criteria for Alzheimer's disease: the IWG-2 criteria. Lancet Neurol. 2014;13(6):614–29.
5. Reitz C, Mayeux R. Alzheimer disease: epidemiology, diagnostic criteria, risk factors and biomarkers. Biochem Pharmacol. 2014;88(4):640–51.
6. Hung SY, Fu WM. Drug candidates in clinical trials for Alzheimer's disease. J Biomed Sci. 2017;24(1):47.
7. Contestabile A. The history of the cholinergic hypothesis. Behav Brain Res. 2011;221(2):334–40.
8. Goldberg AL. Protein degradation and protection against misfolded or damaged proteins. Nature. 2003;426(6968):895–9.
9. Pankiv S, Clausen TH, Lamark T, Brech A, Bruun JA, Outzen H, et al. p62/SQSTM1 binds directly to Atg8/LC3 to facilitate degradation of ubiquitinated protein aggregates by autophagy. J Biol Chem. 2007;282(33):24131–45.
10. Klionsky DJ. The autophagy connection. Dev Cell. 2010;19(1):11–2.
11. Guo F, Liu X, Cai H, Le W. Autophagy in neurodegenerative diseases: pathogenesis and therapy. Brain Pathol. 2018;28(1):3–13.
12. Hung SY, Huang WP, Liou HC, Fu WM. Autophagy protects neuron from Abeta-induced cytotoxicity. Autophagy. 2009;5(4):502–10.
13. Hung SY, Huang WP, Liou HC, Fu WM. LC3 overexpression reduces Abeta neurotoxicity through increasing alpha7nAchR expression and autophagic activity in neurons and mice. Neuropharmacology. 2015;93:243–51.
14. Menzies FM, Fleming A, Caricasole A, Bento CF, Andrews SP, Ashkenazi A, et al. Autophagy and neurodegeneration: pathogenic mechanisms and therapeutic opportunities. Neuron. 2017;93(5):1015–34.
15. Dani JA. Neuronal nicotinic acetylcholine receptor structure and function and response to nicotine. Int Rev Neurobiol. 2015;124:3–19.
16. Russo P, Del Bufalo A, Frustaci A, Fini M, Cesario A. Beyond acetylcholinesterase inhibitors for treating Alzheimer's disease: alpha7-nAChR agonists in human clinical trials. Curr Pharm Des. 2014;20(38):6014–21.
17. Nagele RG, D'Andrea MR, Anderson WJ, Wang HY. Intracellular accumulation of beta-amyloid(1-42) in neurons is facilitated by the alpha 7 nicotinic acetylcholine receptor in Alzheimer's disease. Neuroscience. 2002;110(2):199–211.
18. Wang HY, Lee DH, D'Andrea MR, Peterson PA, Shank RP, Reitz AB. beta-Amyloid(1-42) binds to alpha7 nicotinic acetylcholine receptor with high affinity. Implications for Alzheimer's disease pathology. J Biol Chem. 2000;275(8):5626–32.
19. Keefe RS, Meltzer HA, Dgetluck N, Gawryl M, Koenig G, Moebius HJ, et al. Randomized, double-blind, placebo-controlled study of encenicline, an alpha7 nicotinic acetylcholine receptor agonist, as a treatment for cognitive impairment in schizophrenia. Neuropsychopharmacology. 2015;40(13):3053–60.
20. Rare but severe side effects sideline some Phase 3 Encenicline Trials 2015 [Available from: http://www.alzforum.org/news/research-news/rare-severe-side-effects-sideline-some-phase-3-encenicline-trials.
21. Woodruff-Pak DS, Vogel RW, 3rd, Wenk GL. Galantamine: effect on nicotinic receptor binding, acetylcholinesterase inhibition, and learning. Proc Natl Acad Sci U S A. 2001;98(4):2089–94.
22. Maelicke A, Schrattenholz A, Samochocki M, Radina M, Albuquerque EX. Allosterically potentiating ligands of nicotinic receptors as a treatment strategy for Alzheimer's disease. Behav Brain Res. 2000;113(1–2):199–206.
23. Kihara T, Shimohama S, Sawada H, Honda K, Nakamizo T, Shibasaki H, et al. alpha 7 nicotinic receptor transduces signals to phosphatidylinositol 3-kinase to block A beta-amyloid-induced neurotoxicity. J Biol Chem. 2001;276(17):13541–6.
24. Arias E, Ales E, Gabilan NH, Cano-Abad MF, Villarroya M, Garcia AG, et al. Galantamine prevents apoptosis induced by beta-amyloid and thapsigargin: involvement of nicotinic acetylcholine receptors. Neuropharmacology. 2004;46(1):103–14.
25. Arias E, Gallego-Sandin S, Villarroya M, Garcia AG, Lopez MG. Unequal neuroprotection afforded by the acetylcholinesterase inhibitors galantamine, donepezil, and rivastigmine in SH-SY5Y neuroblastoma cells: role of nicotinic receptors. J Pharmacol Exp Ther. 2005;315(3):1346–53.
26. Yang Z, Klionsky DJ. Mammalian autophagy: core molecular machinery and signaling regulation. Curr Opin Cell Biol. 2010;22(2):124–31.
27. Nixon RA. The role of autophagy in neurodegenerative disease. Nat Med. 2013;19(8):983–97.
28. Sahni S, Merlot AM, Krishan S, Jansson PJ, Richardson DR. Gene of the month: BECN1. J Clin Pathol. 2014;67(8):656–60.
29. Mukherjee UA, Ong SB, Ong SG, Hausenloy DJ. Parkinson's disease proteins: novel mitochondrial targets for cardioprotection. Pharmacology & therapeutics. 2015;156:34–43.
30. Matsuda N, Sato S, Shiba K, Okatsu K, Saisho K, Gautier CA, et al. PINK1 stabilized by mitochondrial depolarization recruits Parkin to damaged mitochondria and activates latent Parkin for mitophagy. J Cell Biol. 2010;189(2):211–21.
31. Gao H, Yang W, Qi Z, Lu L, Duan C, Zhao C, et al. DJ-1 protects dopaminergic neurons against rotenone-induced apoptosis by enhancing ERK-dependent mitophagy. J Mol Biol. 2012;423(2):232–48.
32. Michiorri S, Gelmetti V, Giarda E, Lombardi F, Romano F, Marongiu R, et al. The Parkinson-associated protein PINK1 interacts with Beclin1 and promotes autophagy. Cell Death Differ. 2010;17(6):962–74.
33. Johansen T, Lamark T. Selective autophagy mediated by autophagic adapter proteins. Autophagy. 2011;7(3):279–96.
34. Jonnala RR, Buccafusco JJ. Relationship between the increased cell surface alpha7 nicotinic receptor expression and neuroprotection induced by several nicotinic receptor agonists. J Neurosci Res. 2001;66(4):565–72.
35. Parri HR, Hernandez CM, Dineley KT. Research update: alpha7 nicotinic acetylcholine receptor mechanisms in Alzheimer's disease. Biochem Pharmacol. 2011;82(8):931–42.
36. Ikonomovic MD, Wecker L, Abrahamson EE, Wuu J, Counts SE, Ginsberg SD, et al. Cortical alpha7 nicotinic acetylcholine receptor and beta-amyloid levels in early Alzheimer disease. Arch Neurol. 2009;66(5):646–51.
37. Zhou YY, Li Y, Jiang WQ, Zhou LF. MAPK/JNK signalling: a potential autophagy regulation pathway. Biosci Rep. 2015;35(3).
38. Finlay-Schultz J, Canastar A, Short M, El Gazzar M, Coughlan C, Leonard S. Transcriptional repression of the alpha7 nicotinic

acetylcholine receptor subunit gene (CHRNA7) by activating protein-2alpha (AP-2alpha). J Biol Chem. 2011;286(49):42123–32.
39. Kihara T, Shimohama S, Sawada H, Kimura J, Kume T, Kochiyama H, et al. Nicotinic receptor stimulation protects neurons against beta-amyloid toxicity. Ann Neurol. 1997;42(2):159–63.
40. Yu WH, Cuervo AM, Kumar A, Peterhoff CM, Schmidt SD, Lee JH, et al. Macroautophagy–a novel beta-amyloid peptide-generating pathway activated in Alzheimer's disease. J Cell Biol. 2005;171(1):87–98.
41. Boland B, Kumar A, Lee S, Platt FM, Wegiel J, Yu WH, et al. Autophagy induction and autophagosome clearance in neurons: relationship to autophagic pathology in Alzheimer's disease. J Neurosci. 2008;28(27):6926–37.
42. Klionsky DJ, Cregg JM, Dunn WA, Jr., Emr SD, Sakai Y, Sandoval IV, et al. A unified nomenclature for yeast autophagy-related genes. Dev Cell. 2003;5(4):539–45.
43. Pickford F, Masliah E, Britschgi M, Lucin K, Narasimhan R, Jaeger PA, et al. The autophagy-related protein beclin 1 shows reduced expression in early Alzheimer disease and regulates amyloid beta accumulation in mice. J Clin Invest. 2008;118(6):2190–9.
44. Fang EF, Palikaras K, Sun N, Fivenson EM, Spangler RD, Kerr JS, et al. In vitro and in vivo detection of mitophagy in human cells, *C. elegans*, and mice. J Vis Exp. 2017(129).
45. Lazarou M, Sliter DA, Kane LA, Sarraf SA, Wang C, Burman JL, et al. The ubiquitin kinase PINK1 recruits autophagy receptors to induce mitophagy. Nature. 2015;524(7565):309–14.
46. Wang B, Abraham N, Gao G, Yang Q. Dysregulation of autophagy and mitochondrial function in Parkinson's disease. Transl Neurodegener. 2016;5:19.